This article was downloaded by:
On: *25 January 2011*
Access details: *Access Details: Free Access*
Publisher *Taylor & Francis*
Informa Ltd Registered in England and Wales Registered Number: 1072954 Registered office: Mortimer House, 37-41 Mortimer Street, London W1T 3JH, UK

Liquid Crystals

Publication details, including instructions for authors and subscription information:
http://www.informaworld.com/smpp/title~content=t713926090

Non-symmetric liquid crystal trimers

Peter A. Henderson[a]; Corrie T. Imrie[a]
[a] Department of Chemistry, University of Aberdeen, Aberdeen, UK, AB24 3UE

To cite this Article Henderson, Peter A. and Imrie, Corrie T.(2005) 'Non-symmetric liquid crystal trimers', Liquid Crystals, 32: 6, 673 — 682

To link to this Article: DOI: 10.1080/02678290500116235

URL: http://dx.doi.org/10.1080/02678290500116235

PLEASE SCROLL DOWN FOR ARTICLE

Full terms and conditions of use: http://www.informaworld.com/terms-and-conditions-of-access.pdf

This article may be used for research, teaching and private study purposes. Any substantial or systematic reproduction, re-distribution, re-selling, loan or sub-licensing, systematic supply or distribution in any form to anyone is expressly forbidden.

The publisher does not give any warranty express or implied or make any representation that the contents will be complete or accurate or up to date. The accuracy of any instructions, formulae and drug doses should be independently verified with primary sources. The publisher shall not be liable for any loss, actions, claims, proceedings, demand or costs or damages whatsoever or howsoever caused arising directly or indirectly in connection with or arising out of the use of this material.

Liquid Crystals, Vol. 32, No. 6, June 2005, 673–682

Taylor & Francis
Taylor & Francis Group

Non-symmetric liquid crystal trimers

PETER A. HENDERSON and CORRIE T. IMRIE*
Department of Chemistry, University of Aberdeen, Meston Walk, Aberdeen, UK, AB24 3UE

(*Received 17 July 2004; in final form 10 October 2004; accepted 27 January 2005*)

Four homologous series of non-symmetric linear liquid crystalline trimers, the 4-[(4-{*n*-[4-(4-methoxy-phenylazo)phenoxy]alkyloxy}benzylidene)amino]benzoic acid 6-[4-(4-methoxyphenylazo)phenoxy]hexyl esters, 4-[(4-{*n*-[4-(4-cyanophenylazo)phenoxy]alkyloxy}benzylidene)amino]benzoic acid 6-[4-(4-methoxyphenylazo)phenoxy]hexyl esters, 4-[(4-{*n*-[4-(4-methoxyphenylazo)phenoxy]alkyloxy}benzylidene)amino]benzoic acid 6-[4-(4-cyanophenylazo)phenoxy]hexyl esters and 4-[(4-{*n*-[4-(4-cyanophenylazo)phenoxy]butoxy}benzylidene)amino]benzoic acid 6-[4-(4-cyanophenylazo)phenoxy]hexyl esters, have been synthesized and characterized. In each series one spacer was held constant while the length of the second was varied from 3 to 12 methylene units. All these trimers were nematogenic and exhibited pronounced odd–even effects in both their clearing temperatures and associated entropies. Only two of the trimers exhibited a smectic phase, and specifically those containing two differing terminal mesogenic groups and an undecyl spacer. This strongly suggests the driving force for smectic phase formation is a combination of molecular shape and a specific interaction between unlike mesogenic units. The smectic phase has been assigned as a triply-intercalated alternating smectic C phase, the first example of its kind.

1. Introduction

Liquid crystal trimers consist of molecules containing three mesogenic units joined by two flexible spacers, and are currently attracting increasing interest for two main reasons: first as model compounds for semi-flexible main chain liquid crystal homo- and co-polymers, and second as a new class of liquid crystal oligomers which, by analogy to non-symmetric dimers, are expected to exhibit quite different behaviour from conventional low molar mass mesogens [1–3]. In particular, non-symmetric dimers exhibit intercalated smectic mesophases [1–3], and it is of interest to see if such phases are observed in higher oligomers. Trimers also afford the opportunity specifically to tailor the properties of materials by combining differing functional groups in the same molecule. To harness this potential we must also understand how these materials self-organize.

Non-symmetry can be introduced into the trimeric structure in a variety of ways: for example, non-symmetric trimers may consist of different mesogenic units (either two or all three may differ) [4–9], contain different flexible spacers or terminal chain lengths [10, 11], have different terminal groups, or indeed some combination of all these structural features [12–15]. A study of trimers containing different spacer lengths should enhance our understanding of the role of the spacers in determining liquid crystal behaviour in both oligomers and polymers, while incorporating differing mesogenic groups, specifically, electron rich and electron deficient groups, may lead to the observation of intercalated smectic phases driven by the specific interaction between the unlike mesogenic moieties, as seen for non-symmetric dimers.

In order to explore some of these possibilities we describe here the synthesis and characterization of four homologous series of non-symmetric trimers, see figure 1. In all four series the length of one of the flexible spacers is held constant at six methylene units while the second spacer is varied from $n=3$ to 12 methylene units. It is important to note that the fixed spacer contains an odd number of atoms linking the two mesogenic units, as it is linked by an ester group to the central mesogenic unit. The other three linkages between the spacers and the mesogenic moieties are ether groups. In the MeO6E.*n*OMe and CN6E.*n*CN series the two outer mesogenic moieties are identical, *i.e.* either 4-cyano- or 4-methoxy-azobenzene groups, while the central unit contains a Schiff's base linkage. In the second two series, the terminal mesogenic units also differ: one is an electron rich 4-methoxyazobenzene group and the other an electron deficient 4-cyanoazobenzene group.

---

*Corresponding author. Email: c.t.imrie@abdn.ac.uk

Liquid Crystals
ISSN 0267-8292 print/ISSN 1366-5855 online © 2005 Taylor & Francis Group Ltd
http://www.tandf.co.uk/journals
DOI: 10.1080/02678290500116235

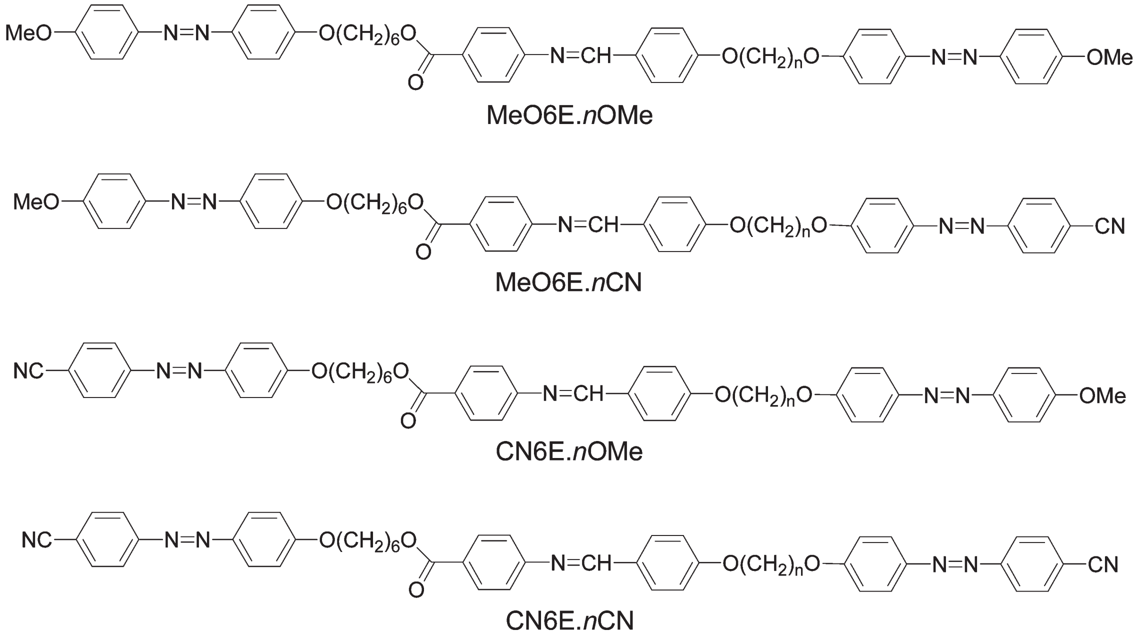

Figure 1. Non-symmetric trimers and their acronyms.

2. Experimental

The synthetic route used to obtain the non-symmetric trimers is shown in the scheme.

2.1. *α-(4-Methoxyazobenzene-4′-oxy)-ω-(4-formylphenyloxy)alkanes, 3 (R′=OMe)*

The synthesis of the α-(4-methoxyazobenzene-4′-oxy)-ω-(4-formylphenyloxy)alkanes, **3**, has been described elsewhere [16].

2.2. *α-(4-Cyanoazobenzene-4′-oxy)-ω-(4-formylphenyloxy)alkanes, 3 (R′=CN)*

The synthesis of the α-(4-cyanoazobenzene-4′-oxy)-ω-(4-formylphenyloxy)alkanes, **3**, is essentially identical to that described for the α-(4-methoxyazobenzene-4′-oxy)-ω-(4-formylphenyloxy)alkanes and thus only spectroscopic data for a representative compound are given. 4-Hydroxy-4′-cyanoazobenzene, **1**, and the α−bromo-ω-(4-cyanoazobenzene-4′-oxy)alkanes, **2**, are synthesized according to the method of Craig *et al.* [17].

1-(4-Cyanoazobenzene-4′-oxy)-3-(4-formylphenyloxy)propane, **3** (R′=CN): ^{1}H NMR ($CDCl_3$) δ (ppm): 9.8 (s, 1H, CHO), 7.9 (m, 4H, Ar–H), 7.8 (m, 4H, Ar–H), 7.0 (m, 4H, Ar–H), 4.2 (t, 4H, $OC\underline{H}_2CH_2$, J=6.0 Hz), 2.3 (qn, 2H, $CH_2C\underline{H}_2CH_2$, J=6.0 Hz). IR (KBr) ν (cm^{-1}): 2223 (CN), 1687 (CO); 1597, 1579, 1509 (Ar–H); 840 (*p*-substituted aromatic).

2.3. *4-Aminobenzoic acid-6-(4-substituted-azobenzene-4′-oxy)-hexyl esters, 4*

The synthesis of the 4-aminobenzoic acid 6-(4-substituted-azobenzene-4′-oxy)hexyl esters, **4**, is shown in the scheme. A representative method is given for the 4-methoxy-substituted derivative together with the spectroscopic data for the 4-cyano-substituted derivative.

4-Aminobenzoic acid-6-(4-methoxyazobenzene-4′-oxy)hexyl ester, **4**, (*R*=OMe): 1-Bromo-6-(4-methoxyazobenzene-4′-oxy)hexane, **2**, (11.7 g, 0.030 mol), 4-aminobenzoic acid (5.50 g, 0.040 mol) and potassium hydrogen carbonate (5.00 g, 0.050 mol) were heated at reflux in DMF (100 ml) with stirring overnight. The reaction mixture was cooled and poured into water (300 ml). The resulting yellow/orange precipitate was collected and recrystallized from ethanol; yield 10.6 g, (79.0 %), m.p. 128°C. ^{1}H NMR ($CDCl_3$) δ (ppm): 7.9 (m, 6H, Ar–H), 7.0 (m, 4H, Ar–H), 6.6 (d, 2H, Ar–H,), 4.3 (t, 2H, $CH_2C\underline{H}_2CO_2$), 4.0 (t, 2H, $OC\underline{H}_2CH_2$), 3.9 (s, 3H, OCH_3), 1.9–1.7 (qn, 4H, $CH_2C\underline{H}_2CH_2CH_2C\underline{H}_2CH_2$), 1.6–1.4 (m, 4H, $CH_2CH_2C\underline{H}_2C\underline{H}_2CH_2CH_2$). IR (KBr) ν (cm^{-1}): 3463, 3375, 1643 (NH_2); 1679 (CO_2); 1596, 1582, 1501 (Ar–H); 1472 (CH_2); 841 (*p*-substituted aromatic).

4-Aminobenzoic acid 6-(4-cyanoazobenzene-4′oxy)-hexyl ester, **4**, (*R*=CN): m.p. Cr–N 142°C, N–I 144°C. ^{1}H NMR ($CDCl_3$) δ (ppm): 8.0–7.7 (m, 8H, Ar–H), 7.0 (d, 2H, Ar–H), 6.6 (d, 2H, Ar–H,), 4.3 (t, 2H,

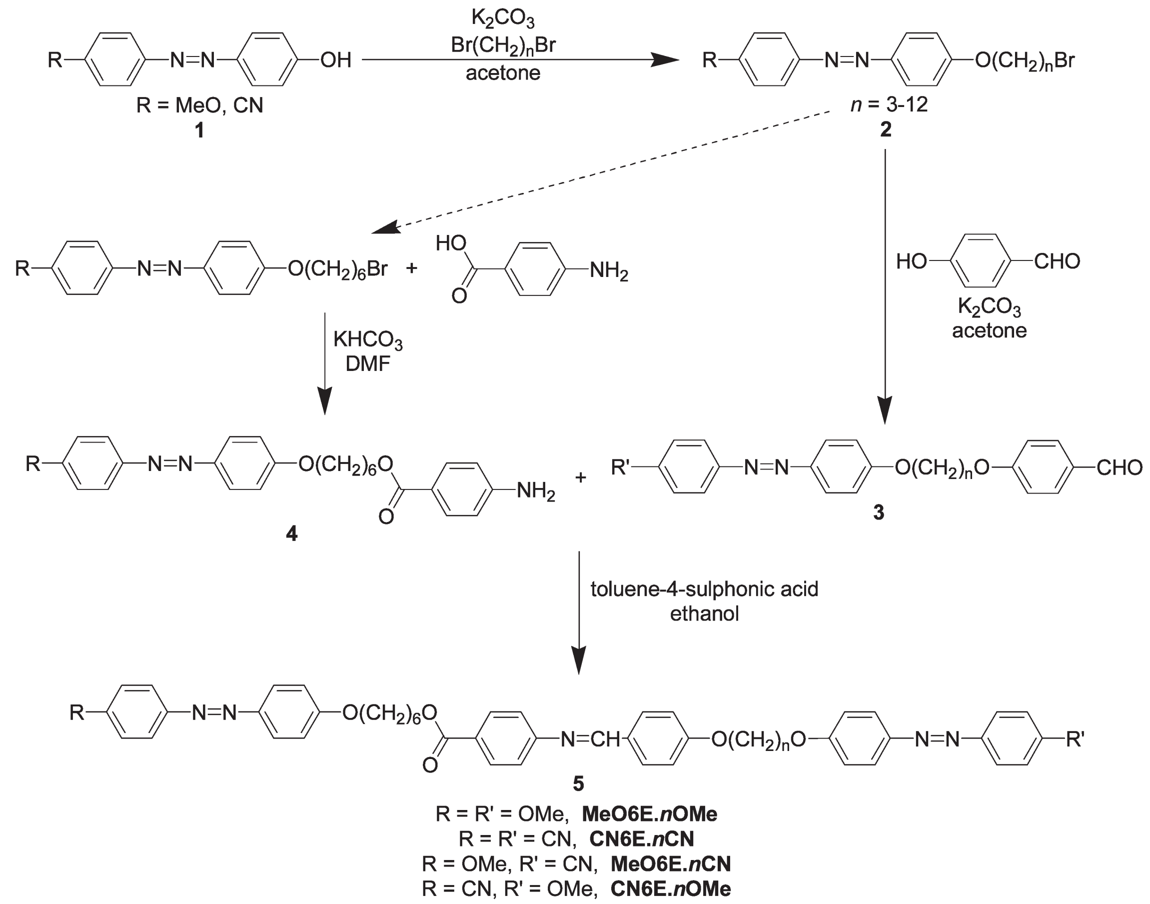

Scheme. Synthesis of non-symmetric liquid crystal trimers.

$CH_2C\underline{H}_2CO_2$), 4.0 (m, 4H, $OC\underline{H}_2CH_2$ and NH_2), 1.9–1.7 (m, 4H, $CH_2C\underline{H}_2CH_2CH_2C\underline{H}_2CH_2$), 1.6–1.4 (m, 4H, $CH_2CH_2C\underline{H}_2C\underline{H}_2CH_2CH_2$). IR (KBr) ν (cm^{-1}): 3466, 3365, 1633 (NH_2); 1686 (CO_2); 1597, 1502 (Ar–H); 850 (*p*-substituted aromatic).

2.4. *Non-symmetric trimers, 5*

The synthesis of the trimers is shown in the scheme. A representative method is given for MeO6E.3OMe. Thus, 1-(4-methoxyazobenzene-4′-oxy)-3-(4-formylphenyloxy)propane, **3** (R'=OMe, n=3), (0.195 g, 0.500 mmol), 4-aminobenzoic acid -6-(4-methoxyazobenzene-4′-oxy)hexyl ester, **4** (R=OMe), (0.224 g, 0.500 mmol) and a catalytic amount of toluene-4-sulphonic acid were heated at reflux in ethanol (25 ml) with stirring overnight. After cooling the resulting yellow precipitate was filtered off and recrystallized twice from toluene; yield 0.202 g, (50.8%). ^{1}H NMR ($CDCl_3$) δ (ppm): 9.9 (s, 1H, CHO); 8.05 (d, 2H, Ar–H, J=8.0 Hz); 7.9–7.8 (m, 10H, Ar–H), 7.05 (d, 2H, Ar–H, J=8.25 Hz); 7.0–6.9 (m, 8H, Ar–H), 6.7 (d, 2H, Ar–H, J=9.0 Hz), 4.4–4.2 (m, 6H, $OC\underline{H}_2CH_2$), 4.1 (m, 2H, $CO_2C\underline{H}_2CH_2$), 3.9 (s, 6H, OCH_3), 2.3 (t, 2H, $OCH_2C\underline{H}_2CH_2O$, J=6.25 Hz) 1.9–1.7 (m, 4H, $CH_2C\underline{H}_2$-$CH_2CH_2C\underline{H}_2CH_2$), 1.6–1.4 (m, 4H, $CH_2CH_2C\underline{H}_2$-$C\underline{H}_2CH_2CH_2$).

2.5. *Characterization and thermal analysis*

All the non-symmetric trimers and their intermediates were characterized by a combination of ^{1}H NMR spectroscopy using a Bruker AC-F 250 MHz spectrometer, FTIR spectroscopy using an ATI Mattson Genesis Series FTIR spectrometer, and elemental analysis carried out by Butterworth Laboratories. The thermal behaviour of the materials was investigated by differential scanning calorimetry (DSC) using a Mettler Toledo DSC 820 differential scanning calorimeter equipped with a TS0801RO sample robot and calibrated using indium and zinc standards. The heating profile in all cases was heat, cool and reheat at 10°C min^{-1} with a 3 min isotherm between heating and cooling. All samples were heated from 0°C to

20–40°C above their clearing temperatures. Thermal data were normally extracted from the second heating trace. Phase characterization was performed by polarising optical microscopy using an Olympus BH2 polarizing microscope equipped with a Linkam TMS 92 hot stage.

3. Results and discussion

3.1. α-*(4-Methoxyazobenzene-4′-oxy)*-ω-*(4-formylphenyloxy)alkanes, 3 (R′=OMe)*

The transition temperatures and associated entropy changes for this series are given in table 1. The butyl, hexyl and undecyl members of this series exhibited an enantiotropic nematic mesophase. Nematic phases throughout this study were identified by the observation of a schlieren texture exhibiting two- and four-point brush disclinations, which flashed when subjected to mechanical stress.

The melting points of the α-(4-methoxyazobenzene-4′-oxy)-ω-(4-formylphenyloxy)alkanes exhibit a large odd–even effect on varying *n*, in which the even members exhibit the higher values, see figure 2. The nematic–isotropic transition temperatures must also exhibit a pronounced alternation on varying *n*, given the absence of liquid crystalline behaviour for the propyl, pentyl and heptyl members. This behaviour is strongly reminiscent of that seen for liquid crystal dimers. The entropy changes associated with the nematic–isotropic transition, $\Delta S_{NI}/R$, for the butyl and hexyl members are similar to those observed for conventional low molar mass mesogens and hence considerably lower than those typically observed for even-membered dimers. By comparison, $\Delta S_{NI}/R$ for the undecyl homologue is much smaller than normally observed for a conventional low molar mass mesogen.

Table 1. Transition temperatures and associated entropy changes for the α-(4-methoxyazobenzene-4′-oxy)-ω-(4-formylphenyloxy)alkanes **3** (R′=OMe).

n	T_{Cr-}/°C	T_{NI}/°C	ΔS_{Cr-}/R	ΔS_{NI}/R
3	146	—	14.3	—
4	154	165	14.5	0.22
5	108	—	13.2	—
6	136	147	16.0	0.26
7	117	—	16.5	—
8	138	—	16.4	—
9	108	—	16.7	—
10	127	—	18.4	—
11	101	107	14.5	0.07
12	123	—	24.1	—

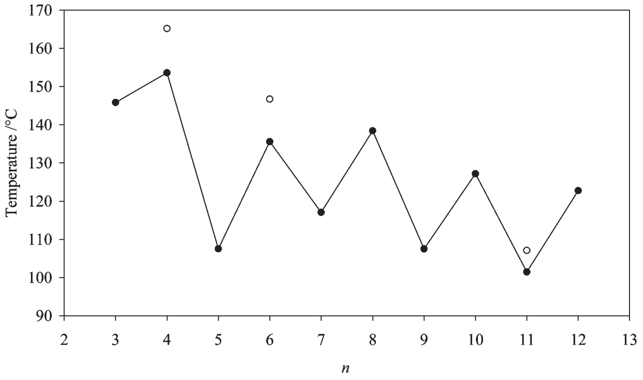

Figure 2. Dependence of the transition temperatures on the length of the flexible spacer, *n*, for the α−(4-methoxyazobenzene-4′-oxy)-ω-(4-formylphenyloxy)alkanes **3** (R′=OMe). (●) Cr–I/Cr–N, (○) N–I.

3.2. α-*Bromo*-ω-*(4-cyanoazobenzene-4′-oxy)alkanes, 2 (R=CN)*

The transition temperatures and associated entropy changes for this series are given in table 2. All the members of this series exhibited a nematic mesophase with the exception of the propyl, butyl and pentyl homologues. The butyl, hexyl, octyl and decyl homologues have been reported previously [18] and the data are in good agreement, except that the SmA phase reported for the octyl member was not observed here.

The dependence of the transition temperatures on the length of the alkyl chain for the α-bromo-ω-(4-cyanoazobenzene-4′-oxy)alkanes is shown in figure 3. The melting points exhibit a pronounced odd–even effect as the chain length is increased, in which the odd members exhibit the higher values. As the terminal chain length is increased an enantiotropic nematic phase emerges at the hexyl member, becoming monotropic on increasing *n* further, see figure 3. An odd–even effect in

Table 2. Transition temperatures and associated entropy changes for the α-bromo-ω-(4-cyanoazobenzene-4′-oxy)alkanes **2** (*R*=CN). Monotropic phases are given in brackets and were obtained from DSC cooling curves.

n	T_{Cr-}/°C	T_{NI}/°C	ΔS_{CrN}/R	ΔS_{NI}/R
3	146	—	8.43	—
4	123	—	8.89	—
5	136	—	10.18	—
6	91	103	9.48	0.03
7	118	121	8.55[a]	
8	96	100	8.88	0.04
9	115	(96)	11.25[a]	
10	105	(94)	14.77	0.04
11	116	(96)	12.47[a]	
12	105	(81)	11.58	0.05

[a] Combined melting and clearing entropy change because the DSC peaks could not be resolved.

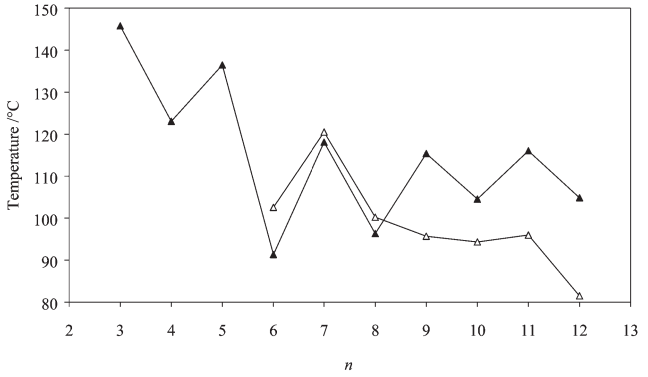

Figure 3. Dependence of transition temperatures on the length of the alkyl chain, *n*, for the α-bromo-ω-(4-cyanoazobenzene-4′-oxy)alkanes **2** (*R*=CN). (▲) Cr–I/Cr–N, (△) N–I.

T_{NI} is evident initially, in which members with *n* odd have the higher values, although T_{NI} for the nonyl member appears to be rather low. Considering the total number of atoms in the chain, it would appear that the terminal bromine atom is behaving like a methyl group, otherwise an odd–even effect having the opposite sense would be expected. This is in direct contrast to the behaviour of the α-bromo-ω-(4-methoxyazobenzene-4′-oxy)alkanes (**2**, *R*=OMe), for which the bromine atom does not appear to play a significant role in determining the sense of the odd–even effect [19]. The physical significance of this observation is not clear. The entropy changes for the clearing transitions exhibited by the even members are very small, see table 2, while for the odd members the melting and clearing peaks could not be separated.

3.3. *α-(4-Cyanoazobenzene-4′-oxy)-ω-(4-formylphenyloxy)alkanes, 3 (R′=CN)*

The transition temperatures and associated entropy changes for this series are given in table 3. All the members of this series exhibit an enantiotropic nematic mesophase.

Table 3. Transition data for the α-(4-cyanoazobenzene-4′-oxy)-ω-(4-formylphenyloxy)alkanes **3** (*R*′=CN).

n	T_{CrN}/°C	T_{NI}/°C	ΔS_{CrN}/R	ΔS_{NI}/R
3	155	158	10.1[a]	
4	123	155	7.05	0.66
5	110	113	8.86	0.30
6	116	142	8.71	0.72
7	100	107	8.71	0.42
8	104	133	10.1	0.82
9	86	112	11.0	0.47
10	111	123	12.8	1.02
11	80	112	11.3	0.53
12	110	114	13.1	1.26

[a] Combined melting and clearing entropy change.

The dependence of transition temperature on the length of the alkyl spacer is shown in figure 4. The melting points exhibit an odd–even effect in which the even members show the higher values, although the melting point of the propyl member is rather higher than expected. The clearing temperatures also exhibit an odd–even effect which is attenuated on increasing *n*; again the clearing temperature of the propyl member is surprisingly high. Only three members of the α-(4-methoxyazobenzene-4′-oxy)-ω-(4-formylphenyloxy)alkane series were liquid crystalline, see figure 2, and this reflects their higher melting points but similar clearing temperatures when compared with the corresponding cyano-substituted materials. The entropy change associated with the clearing transition, ΔS_{NI}/R, for this series exhibits a pronounced odd–even effect as *n* is increased, in which even members have values typically twice as large as those of the odd members. It is interesting to note that these 4-cyano-substituted materials exhibit considerably higher clearing entropies than the corresponding 4-methoxy-substituted homologues. The reasons for this are unclear.

3.4. *MeO6E.***n***OMe series*

The transition temperatures and associated entropy changes for the MeO6E.*n*OMe series are given in table 4. All members of this series exhibited an enantiotropic nematic phase.

The dependence of the transition temperatures on the number of methylene units, *n*, in the flexible spacer is shown in figure 5. Both the melting and clearing temperatures exhibit an odd–even effect, in which the even members have the higher temperatures. There is a marked attenuation of the odd–even effect seen for T_{NI}

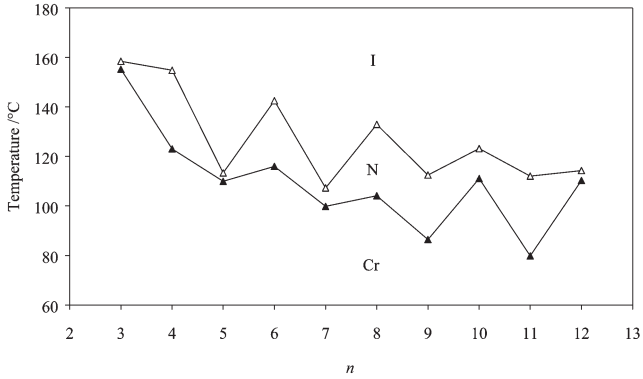

Figure 4. Dependence of the transition temperatures on the length of the flexible spacer, *n*, for the α−(4-cyanoazobenzene-4′-oxy)-ω-(4-formylphenyloxy)alkanes **3** (R′=CN). (▲) Cr–N, (△) N–I.

Table 4. Transition temperatures and associated entropy changes for the MeO6E.*n*OMe series.

n	T_{CrN}/°C	T_{NI}/°C	ΔS_{CrN}/R	ΔS_{NI}/R
3	140	159	11.5	0.35
4	171	235	21.6	1.43
5	159	194	18.2	0.56
6	167	210	26.5	1.31
7	155	185	19.0	0.62
8	163	204	21.6	1.44
9	154	180	19.5	0.87
10	161	191	23.3	1.47
11	138	178	18.6	0.92
12	159	182	21.1	1.52

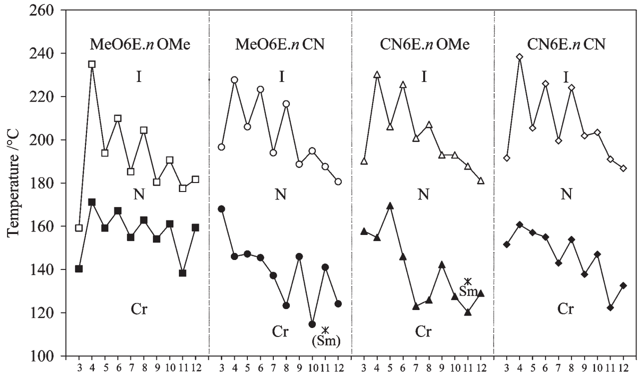

Figure 5. Dependence of the transition temperatures on the number of methylene units, *n*, in the variable flexible spacer, for the four trimer series. Closed symbols represent crystal–nematic and open symbols nematic–isotropic transition temperatures. * Denotes Sm–N transition temperatures.

on increasing *n*. The transition temperatures for MeO6E.3OMe are slightly lower than may be expected. This is presumably because the large difference in spacer lengths combined with the highly non-linear shape arising from the propyl spacer inhibits efficient packing of the molecules in either the crystal or liquid crystal phase. An interpretation of the odd–even effect seen for T_{NI} and its attenuation on increasing *n* will be given later for all four non-symmetric trimer series.

The nematic–isotropic entropy change also exhibits an odd–even effect which does not attenuate on increasing *n*, see figure 6.

3.5. *MeO6E.*n*CN series*

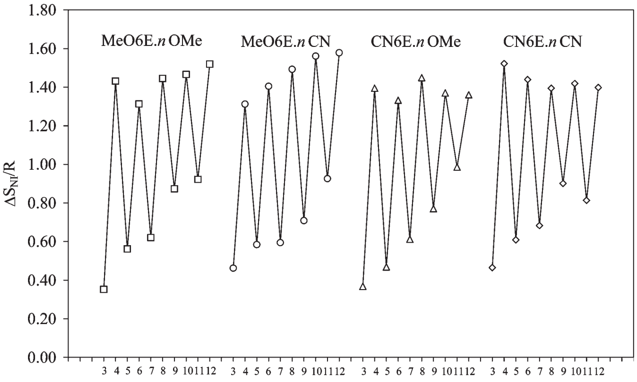

Figure 6. Dependence of the nematic–isotropic entropy on the number of methylene units, *n*, in the variable flexible spacer for the four trimer series.

Table 5. Transition temperatures and associated entropy changes for the MeO6E.*n*CN series.

n	T_{CrN}/°C	T_{NI}/°C	ΔS_{CrN}/R	ΔS_{NI}/R
3	168	197	20.2	0.46
4	146	228	12.4	1.31
5	147	206	19.1	0.58
6	146	223	14.5	1.40
7	137	194	14.8	0.59
8	123	217	18.4	1.49
9	146	189	17.0	0.71
10	115	195	13.4	1.56
11[a]	141	188	21.8	0.93
12	124	181	10.7	1.58

[a] T_{NSm}=112°C, ΔS_{NSm}/R=1.05.

The transition temperatures and associated entropy changes for the MeO6E.*n*CN series are given in table 5. All the members of this series exhibit an enantiotropic nematic phase. In addition MeO6E.11CN exhibits a monotropic smectic phase. On cooling from the nematic phase a texture consisting of slightly rounded focal-conic fans is obtained, see figure 7, which shears to give a schlieren texture. The monotropic nature of the phase precluded further study. The structure of this phase will be discussed later.

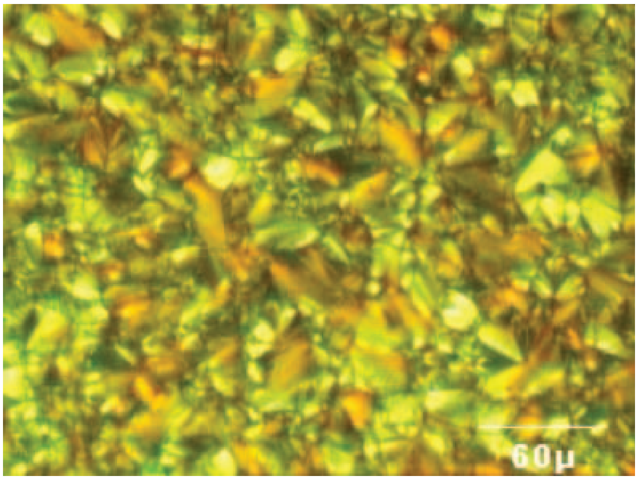

Figure 7. Focal conic fan texture of MeO6E.11CN at 110°C.

Figure 5 shows the dependence of the transition temperatures on *n*, the length of the variable spacer for the MeO6E.*n*CN series. The melting points initially show an irregular dependence on *n* but an alternation appears on further increasing *n* in which the odd members exhibit the higher values. The clearing temperatures again exhibit an odd–even effect in which even members show the higher values and which is attenuated on increasing *n*. The dependence of the clearing entropy on *n* is shown in figure 6 and an odd–even effect is seen which is only slightly attenuated as *n* is increased.

3.6. *CN6E.*n*OMe series*

The transition temperatures and associated entropy changes for the CN6E.*n*OMe series are given in table 6. All the members exhibit an enantiotropic nematic phase and CN6E.11OMe also shows an enantiotropic smectic phase [20].

The smectic phase of CN6E.11OMe exhibits a texture consisting of well -defined focal-conic fans which shear to give a schlieren texture. A thin film of the smectic phase, and cooling regions of homeotropically aligned nematic phase obtained using a cleaned glass slide, give schlieren textures indicating a tilted phase. Both two- and four-point disclinations are observed in the homeotropic region implying the presence of an alternating tilted phase [21, 22].

The X-ray diffraction pattern obtained for the smectic mesophase contained one diffraction peak in the low angle region and a diffuse band in the wide angle region. The low angle peak gave a *d*-spacing of just 19.0 Å compared with the calculated molecular length of 60.4 Å. These data strongly suggest the formation a triply-intercalated alternating smectic C phase, see figure 8, and this has been described in detail elsewhere [20]. Recently three trimers were reported which exhibited a monolayer SmC phase with an alternation of the tilt angle between the layers; *i.e.* an anticlinic SmC phase [23].

Table 6. Transition temperatures and associated entropy changes for the CN6E.*n*OMe series.

n	T_{CrN}/°C	T_{NI}/°C	$\Delta S_{\mathrm{CrN}}/R$	$\Delta S_{\mathrm{NI}}/R$
3	158	190	16.2	0.37
4	155	230	13.1	1.39
5	170	206	23.0	0.47
6	146	226	18.0	1.33
7	123	201	14.6	0.61
8	126	207	16.7	1.45
9	142	193	19.4	0.77
10	128	193	17.4	1.37
11	120[a], 134[b]	188	16.4[a], 1.60[b]	0.99
12	129	181	20.4	1.36

[a] T_{CrSm}/°C, $\Delta S_{\mathrm{CrSm}}/R$. [b] T_{SmN}/°C, $\Delta S_{\mathrm{SmN}}/R$.

Figure 8. Schematic representation of the triply-intercalated alternating smectic C phase exhibited by CN6E.11OMe.

The driving force for the formation of this smectic modification was suggested to be favourable electrostatic interactions between unlike mesogenic groups and the ability of the bent odd-membered molecules to pack efficiently in the alternating structure. An equimolar mixture of MeO6E.11OMe and CN6E.11CN exhibits an induced smectic phase, see figure 9, although its monotropic nature precluded its study using X-ray diffration.

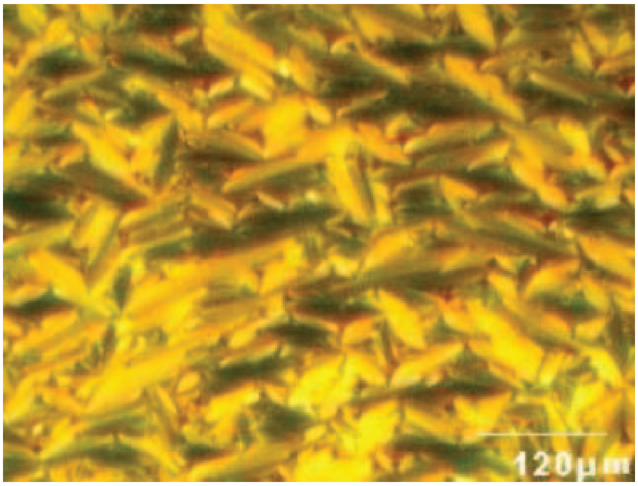

Figure 9. Focal conic fan texture exhibited by the 1:1 mixture of MeO6E.11OMe and CN6E.11CN at 105°C.

Table 7. Transition temperatures and associated entropy changes for the CN6E.*n*CN series.

n	T_{CrN}/°C	T_{NI}/°C	ΔS_{CrN}/R	ΔS_{NI}/R
3	152	192	8.2	0.47
4	161	238	14.6	1.52
5	157	205	13.6	0.61
6	155	226	14.5	1.44
7	143	200	14.9	0.68
8	154	224	17.1	1.39
9	138	202	14.9	0.90
10	147	203	18.9	1.42
11	122	191	13.6	0.81
12	133	187	16.0	1.40

The melting temperatures of the CN6E.*n*OMe series do not exhibit a regular dependence on *n*, see figure 5. By comparison the clearing temperatures do exhibit an odd–even effect which attenuates strongly with increasing *n*, see figure 5, and indeed the clearing temperature of $n=12$ is below that of $n=11$. The clearing entropy changes, see figure 6, also exhibit an odd–even effect. The entropy values remain relatively constant for even values of *n*, whereas the values increase with increasing *n* for odd values, resulting in an attenuation of the odd–even effect.

3.7. *CN6E.*n*CN series*

All the members of the CN6E.*n*CN series exhibit an enantiotropic nematic phase; the transition temperatures and associated entropy changes are given in table 7. The dependence of the transition temperatures on *n* for the CN6E.*n*CN series is shown in figure 5. A weak odd–even effect is observed for the melting temperatures which becomes more pronounced as *n* is increased. An odd–even effect is also seen for the clearing temperatures, which attenuates with increasing *n*. As with the MeO6E.*n*OMe and CN6E.*n*OMe series the clearing temperature for $n=12$ is below that for $n=11$. The dependence of the clearing entropy change on *n* is shown in figure 6, and again an odd–even effect is seen. For even values of *n* ΔS_{NI}/R appears almost constant, whereas the value increases with increasing odd values of *n*, resulting in an attenuation of the alternation.

3.8. *Comparison of the four non-symmetric trimer series*

The dependences of the melting points on the length of the variable flexible spacer for each series can be compared in figure 5. There is no apparent trend between the series although the MeO6E.*n*OMe series generally exhibits the highest melting points. The clearing temperatures for the four series can also be compared in figure 5 and each series exhibits an odd–even effect. The CN6E.*n*CN series generally exhibits the highest clearing temperatures and the MeO6E.*n*OMe series the lowest. The trimers containing two differing outer mesogenic groups typically show clearing temperatures between those of the trimers containing identical outer mesogenic groups. We will return to this observation later.

Figure 6 compares the clearing entropies of the four series and for each a pronounced odd–even effect is observed. The values of the clearing entropies are rather similar between the series and no trend in behaviour is apparent.

We have seen that all four series of trimers exhibit an odd–even effect in their clearing temperatures, which is attenuated on increasing the length of one of the flexible spacers, see figure 5. An interpretation of the odd–even effect seen for the clearing temperatures of symmetric trimers [6, 24] and dimers [1–3] on varying spacer length, in terms of the dependence of shape on the parity of the spacers, has been discussed previously and presumably may also be applied here. This approach developed by Luckhurst and co-workers to model the properties of dimers [3, 11] has also been used successfully to account for the behaviour of symmetric trimers [25]. The magnitude of the odd–even effect observed in the clearing temperature for any one of the four series is smaller than that seen for symmetric trimer series in which both spacers are varied [6, 24]. The reason for this, quite simply, is that the fixed spacer reduces the extent of the average shape change, see figure 10. Thus, the change in the average molecular shape on varying the length of just one spacer is less pronounced compared with trimers containing two variable spacers. It is also apparent that the clearing entropies for these series are considerably lower than those of odd-membered symmetric trimers, suggesting

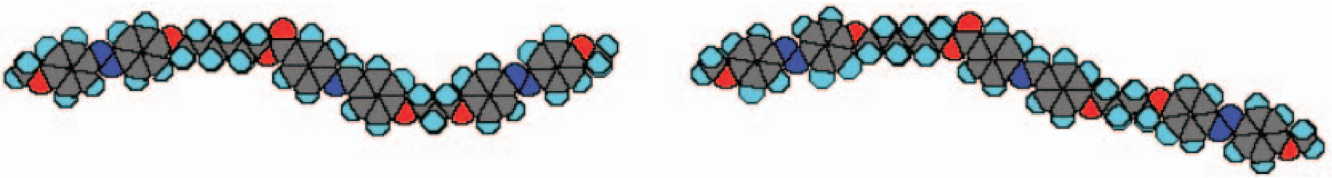

Figure 10. Molecular shapes of (*a*) an odd (MeO6E.3OMe) and (*b*) an even (MeO6E.4OMe) membered trimer.

that the mismatch in spacer length reduces the interaction strength parameters between the mesogenic units.

If the fixed spacer contained an even number of connecting atoms then it would be reasonable to assume that all the clearing temperatures and associated entropy changes would be higher than those seen for these series due to the enhanced shape anisotropy and increased interaction strength parameters. Such behaviour is indeed observed for non-symmetric trimers reported by Barnes and Luckhurst [10, 11]:

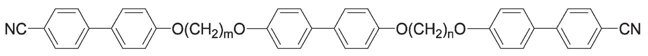

m,n trimer series

In order to investigate the effects of *n* and terminal group substitution on the clearing temperature, the relative magnitudes of the deviations of the clearing temperatures of the two series with non-identical terminal groups (MeO6E.*n*CN and CN6E.*n*OMe), T_{AB}, were compared with the mean of those from the two series with identical terminal groups (T_A and T_B), in terms of a scaled deviation defined as [26]:

$$\Delta T_{SC} = \frac{2T_{AB} - (T_A + T_B)}{(T_A + T_B)}$$

The dependence of ΔT_{SC} on *n* for the two series of non-symmetric trimers is shown in figure 11. ΔT_{SC} for the CN6E.*n*OMe series are generally slightly higher than for those of the MeO6E.*n*CN series. While there is a tendency for the two series of trimers with non-identical terminal groups to have clearing temperatures higher than the average of the two series with similar terminal groups, this is not observed across the complete range of spacer lengths. This presumably indicates that the interaction between the unlike groups is to some extent controlled by the relative length of the spacers. We must note, however, that all the ΔT_{SC} values are small and it would be unwise to comment further on their molecular significance.

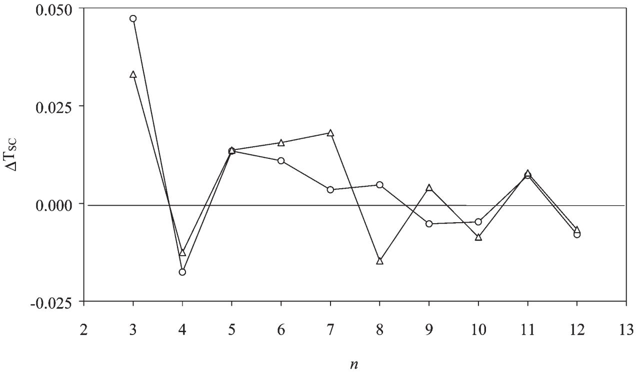

Figure 11. Scaled clearing temperature deviations for MeO6E.*n*CN (○) and CN6E.*n*OMe (△).

4. Conclusions

Four series of non-symmetric liquid crystal trimers have been synthesized and characterized. In each series one spacer was held constant whilst the other was varied from 3 to 12 methylene units. Non-symmetry was also introduced into the structure by incorporating different terminal groups. All four series exhibited the nematic phase with an odd–even effect seen in the clearing temperatures and entropy values on increasing the length of the variable spacer. Two compounds exhibited a smectic phase. The structure of the smectic phase, based on optical microscopy and the layer spacing, is proposed to be a triply-intercalated alternating smectic C phase. The driving force for the formation of this smectic phase is believed to be a combination of molecular shape and specific interactions between the three unlike mesogenic units. This is believed to be the first example of such a triply-intercalated alternating smectic C phase seen for liquid crystal trimers. Further work on non-symmetric and symmetric trimers is now required to understand more fully how the transitional properties of oligomers evolve into those of polymers.

References

[1] C.T. Imrie, P.A. Henderson. *Curr. Opin. colloid inter. Sci.*, **7**, 298 (2002).
[2] C.T. Imrie. *Struct. Bond.*, **95**, 149 (1999).
[3] C.T. Imrie, G.R. Luckhurst. *Handbook of Liquid Crystals.* Vol. 2B, D. Demus, J.W. Goodby, G.W. Gray, H.W. Spiess, V. Vill (Eds), p. 801, Wiley-VCH, Weinheim (1998).
[4] R. Centore, A. Roviello, A. Sirigu. *Mol. Cryst. liq. Cryst.*, **182B**, 233 (1990).
[5] T. Ikeda, T. Miyamoto, S. Kurihara, M. Tsukada, S. Tazuke. *Mol. Cryst. liq. Cryst.*, **182B**, 357 (1990).
[6] C.T. Imrie, G.R. Luckhurst. *J. mater. Chem.*, **8**, 1339 (1998).
[7] S. Mahlstedt, D. Janietz, C. Schmidt, A. Stracke, J.H. Wendorff. *Liq. Cryst.*, **26**, 1359 (1999).
[8] S. Mahlstedt, D. Janietz, A. Stracke, J.H. Wendorff. *Chem. Commun.*, **1**, 15 (2000).
[9] W. Kreuder, H. Ringsdorf, O. Herrmann-Schönherr, J.H. Wendorff. *Angew. Chem. int. Ed. Engl.*, **26**, 1249 (1987).
[10] P.J. Barnes. PhD. thesis, University of Southampton, UK (1994).
[11] G.R. Luckhurst. *Macromol. Symp.*, **96**, 1 (1995).
[12] A.T.M. Marcelis, A. Koudijs, E.J.R. Sudhölter. *Liq. Cryst.*, **18**, 851 (1995).
[13] A.T.M. Marcelis, A. Koudijs, E.J.R. Sudhölter. *Liq. Cryst.*, **21**, 87 (1996).
[14] C.V. Yelamaggad, U.S. Hiremath, D.S. Shankar Rao, S. Krishna Prasad. *Chem. Commun.*, **1**, 57 (2000).

[15] C.V. Yelamaggad, S. Anitha Nagamani, U.S. Hiremath, D.S. Shankar Rao, S. Krishna Prasad. *Liq. Cryst.*, **28**, 1581 (2001).

[16] P.A. Henderson, R.T. Inkster, J.M. Seddon, C.T. Imrie. *J. mater. Chem.*, **11**, 2722 (2001).

[17] A.A. Craig, I. Winchester, P.C. Madden, P. Larcey, I.W. Hamley, C.T. Imrie. *Polymer*, **39**, 1197 (1998).

[18] J.V. Crivello, M. Deptolla, H. Ringsdorf. *Liq. Cryst.*, **3**, 235 (1988).

[19] C.T. Imrie, F.E. Karasz, G.S. Attard. *Macromol.*, **25**, 1278 (1992).

[20] P.A. Henderson, C.T. Imrie, J.M. Seddon. *J. mater. Chem.*, **14**, 2486 (2004).

[21] J. Watanabe, H. Komura, T. Niori. *Liq. Cryst.*, **13**, 455 (1993).

[22] Y. Takanishi, H. Takezoe, A. Fukuda, K. Hidehiro, J. Watanabe. *J. mater. Chem.*, **2**, 71 (1992).

[23] I. Nishiyama, J. Yamamoto, J.W. Goodby, H. Yokoyama. *J. mater. Chem.*, **13**, 2429 (2003).

[24] P.A. Henderson, A.G. Cook, C.T. Imrie. *Liq. Cryst.*, **31**, 1427 (2004).

[25] M. Vacatello. *Macromol. Theory Simul.*, **11**, 501 (2002).

[26] G.S. Attard, R.W. Date, C.T. Imrie, G.R. Luckhurst, S.J. Roskilly, J.M. Seddon, L. Taylor. *Liq. Cryst.*, **16**, 529 (1994).